Title

Amphoteric Soy Protein-Rich Fibers for Rapid and Selective Adsorption and Desorption of Ionic Dyes

Journal

ACS Omega, 5(1)

ISSN

2470-1343

Authors

Liu, Xingchen
Hsieh, You-Lo

Publication Date

2020-01-14

DOI

10.1021/acsomega.9b03242

Peer reviewed

ACS OMEGA

Article

Cite This: ACS Omega 2020, 5, 634−642

http://pubs.acs.org/journal/acsodf

Amphoteric Soy Protein-Rich Fibers for Rapid and Selective Adsorption and Desorption of Ionic Dyes

Xingchen Liu and You-Lo Hsieh*

Biological and Agricultural Engineering, University of California, Davis, 95616 California, United States

Supporting Information

ABSTRACT: Uniquely amphoteric soy protein (SP)-rich ultra-fine fibers (231 nm average diameter) have been facilely electrospun from aq. colloids and rendered water-insoluble by heating (150 °C, 12 h) to be highly stable over 14 d (pH 7) as well as under extremely acidic to basic (pH 0−10, 2 d) or at boil (2 h) conditions. The SP-rich fibrous membranes are easily tuned to be charged either negatively by deprotonation above or positively by protonation below the 4.5 PI of SPs. This pH-responsive amphoterism has been demonstrated for rapid adsorption of either cationic or anionic dyes, selective adsorption of either dye from their mixtures, and repetitive adsorption/desorption to recover and reuse both dyes and membranes. Chemisorption and heterogeneous adsorption of ionic dyes was confirmed by close fitting to the pseudo-second-order kinetic model (R^2 = 0.9977−0.9999) and Freundlich adsorption isotherm (R^2 = 0.9879). This is the first report of water-resilient and pH-robust ultrafine fibrous membranes fabricated from aqueous colloids of neat globular SPs, the major byproducts of under-utilized edible oil and biodiesel. The natural polyampholyte origin, amphoterism, and green processing make these fibrous materials unique and versatile for many potential applications involving both anionic and cationic species.

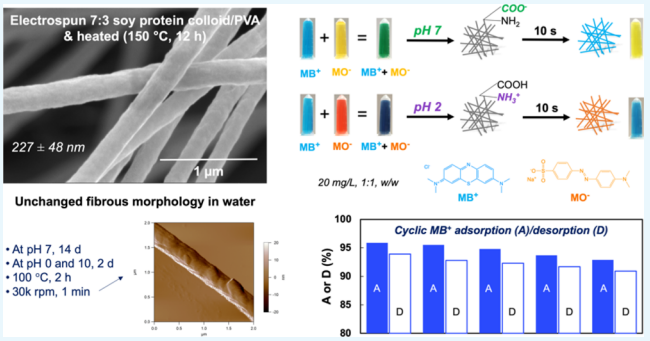

INTRODUCTION

The increasing and cumulative presence of dyes from industrial effluents in our water ways has posed serious toxicity to aquatic ecosystems and human health.[1] To remove dyes, activated carbon particulates[1] and biosorbents derived from agricultural byproducts[2] are among the most widely studied, however, still produce concentrated sludges as secondary pollutants that require safe disposal and/or costly recycling. Polymeric adsorbents that are capable of controlled separation and regeneration of valuable dyes are thus appealing.[3,4] Either negatively or positively charged synthetic[5−10] and natural[11−13] polyelectrolytes have been processed into adsorbents for selectively adsorbing either cationic[5,9,11−13] or anionic[6−8,10] dyes. Some pH-responsive adsorbents have been derived but only from synthetic polyampholytes[14] and mixtures with various chemical modification and/or polymerization.[15−19] None has been generated from natural polymers or polyampholytes, that is, proteins, especially in the form of ultrafine fibers.

Soy proteins (SPs) are mixtures of large and complex globular proteins with ca. 47 mol % amino acids containing strongly polar side groups, that is, 20.5 mol % −COOH and 18.0 mol % $-NH_2$,[20] thus natural polyampholytes. Epichlorohydrin-crosslinked SP hydrogels have shown to exhibit pH-responsive swelling behavior at pH 2−12.[21] SPs are also readily available, being 44−48% of the vastly under-utilized soy meals, that is, the main byproduct of the largest edible oil and biodiesel production in the United States.[22] Among adsorbents, fibers are desirable for their high specific surface and easy engineering into porous and continuous mass. Fiber spinning the complex and large globular SPs is, however, challenging in comparison to fibrous proteins, such as collagen[23] and silk fibroin.[24] To electrospin into finer fibers for even a higher specific surface, SPs were denatured and hydrolyzed by heat (40−90 °C, 40 min to 8 d)[25−30] and/or alkali (pH 12)[27,29,31] to be dispersed in organic[25,26] or aqueous media[27−31] first, then with added polymer carriers, such as polyethylene oxide (400−900 *k*Da at 10 w/w %[27,31] or 200 *k*Da at 33 w/w %[25,26]) and polyvinyl alcohol (PVA) (78[29] or 100[28] *k*Da at 50 w/w %), and/or surfactants (i.e. 0.5[29] or 1%[27] Triton X-100 and 17.5% sodium dodecyl sulfate[30]).

Previously, we have successfully dispersed soy protein isolate (SPI) homogeneously as aqueous (aq.) SP colloids (SPCs) at up to 9% by high-speed blending (30k rpm, 15 min).[32] These aq. SPCs have shown to be amphoteric, exhibiting ζ-potential ranging from −39.4 to +32.4 mV and an isoelectric point (PI) of 4.5. This study was, therefore, to develop a green and facile approach to process these unmodified aq. SPCs into high specific surface fibrous membranes. First, electrospinning of aq. SPCs was investigated by hybridizing with fiber-forming PVA

Received: October 1, 2019
Accepted: November 28, 2019
Published: December 23, 2019

DOI: 10.1021/acsomega.9b03242
ACS Omega 2020, 5, 634−642

to avoid organic reactions or chemical modification. The highly polar SP and PVA were then rendered less water soluble by cross-linking via chemical reaction with naturally occurring, biocompatible, and less harmful genipin, that is, 5000−10000 times less cytotoxic than glutaraldehyde[33] and has shown to cross-link electrospun chitosan (21 °C, 1 d)[34] and gelatin (21 °C, 7 d)[35] fibers. In addition, heat-induced self-condensation of amino acid side groups (105−180 °C, 24−120 h)[36−38] that have demonstrated to render electrospun collagen[36,37] and gelatin[38] fibers water insoluble was streamlined. The effects of genipin cross-linking and streamlined heat treatment were systematically evaluated by aq. solubility and resiliency as well as the secondary structure of SPs, crystalline domains, chemical changes, and thermal behaviors. The pH-tunable amphoteric characteristics of the optimally cross-linked membranes were elucidated by their selective adsorption of cationic and anionic dyes as well as the adsorption isotherm and kinetics, and cyclic adsorption/desorption for dye recovery as well as fibrous membrane regeneration and reuse.

RESULTS AND DISCUSSION

Electrospinnability of Alkaline- and Heat-Treated SPs and SPCs. Aqueous (aq.) 9% SP control suspension that was magnetically stirred for 1 h phase separated in hours and could only be electrosprayed into droplets. Adding equal mass of 9% PVA to the aq. SP control enabled electrospinning only at a very low 0.01 mL/h rate and produced mostly beads with very few fibers, while dripped continuously (Figure S1, Table S1). Heating (90 °C, 45 min) aq. SP control caused gelation that was attributed to denaturation or the unfolding of globular structures to reduce exposure of hydrophobic moieties to water. Following pH adjustment to 12, the gel became miscible with equal mass of PVA but still generated mostly beads stringing along thin fibers (Figure S1). Treating aq. SP control in the reverse order, that is, adjusting pH to 12 then heating at 90 °C for 45 min, enabled continuous electrospinning of 1:1 SP/PVA mixture at 1.5 mL/h for at least 20 h without any dripping into a white membrane composed of uniform, straight, and smooth fibers with the average diameter of 267 nm (±65 nm, N = 100) (Figure S1). Heating the basic adjusted SP control also enable electrospinning with less PVA, but 7:3 SP/PVA(9.75%) fibers were irregular in widths and among lots of beads and splashes (Figure S1). This mixture also phase separated in 7−8 h to prevent continuous electrospinning. Both the heterogenous electrospun products and phase separation indicated the instability of the mixture.

In contrast, aq. SPC, the supernatant from high speed blending, mixed with PVA at 7:3 mass ratio could be facilely electrospun at 1.5−2 mL/h feeding rate continuously for at least 20 h. The fibrous membrane appeared white initially and then became pale yellow when thickened. Fibers were uniform in 231 nm (±46 nm, N = 100) width with slightly angulated surfaces (Figure 1a). Further increasing SPC in the mixture to 90% could also be electrospun continuously, but beads were observed regularly spaced along much thinner fibers (Figure 1b). The significantly improved electrospinnability of SPC mixtures is attributed to the surface-active behavior of aq. SPCs that have shown to reduce the surface tension of water to 41.2 mN/m at above 0.98%.[32] The presence of residual salts from alkali extraction and acid precipitation of SPI isolations may also increase the net charge density to aid electrospinning. These most uniform 7:3 SPC/PVA hybrid fibrous membranes were therefore selected for further studies and denotes simply as fibrous membranes from here on.

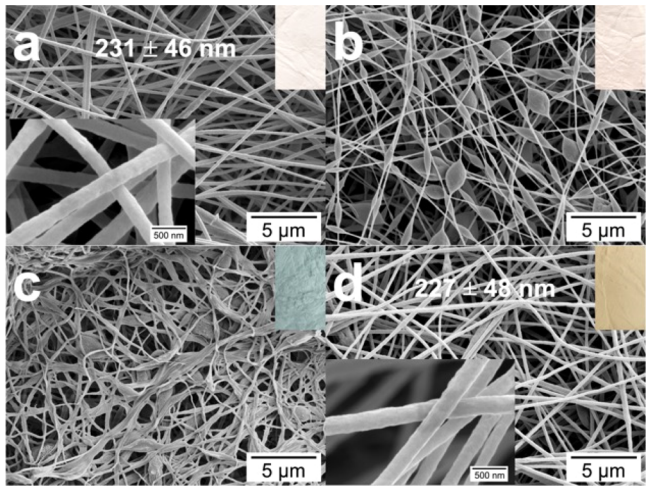

Figure 1. SEM images of electrospun SPC/PVA fibrous membranes: (a) as-spun 7:3; (b) as-spun 9:1; (c) genipin-reacted (65 °C, 1 h) and lyophilized 7:3; (d) heated (150 °C, 12 h) 7:3. Photograph of membrane is shown as inset in each.

Genipin Reaction and Heat Treatment. The 7:3 SPC/PVA fibrous membranes were chemically cross-linked with 11 mM genipin in 1:1 v/v EtOH/water under two conditions or heat-treated (150 °C, 12 h). Complete submersion in genipin solutions at ambient temperature turned the top of the membrane yellowish initially, then some pale blue spots appeared after 5 h, and all dark blue after 24 h; while the bottom remained pale blue (Figure S2), probably because of the lack of access to oxygen. The membrane saturated with genipin solutions at 65 °C appeared bluish in 15 min, then dark blue on both sides in 30−60 min (Figure S2) and, upon lyophilization, became a pale blue and fluffy mass of irregularly sized, deformed, and merged fibers (Figure 1c). The heat-treated membrane, on the other hand, retained the same fiber sizes (227 ± 48 nm, N = 100) and morphology but became slightly pale brown (Figure 1d). The brownish color may be attributed to the formation of melanoidin pigments via Maillard reactions between amines of SPs and carbonyl groups of reducing sugars, that is, glucose and lactose, known to be present in SPI. Primary amines of SPs may either react with the genipin ester group via SN_2 nucleophilic substitution to form secondary amides or attack the olefinic C-3 carbon of genipin nucleophilically to open the dihydropyran ring to heterocyclic tertiary amine intermediate 1, and then into intermediate 2 after removing the C-10 hydroxyl (Figure S2). Aided by oxygen radicals, these intermediates have shown to polymerize into blue color products that are commonly recognized as indication of successful genipin cross-linking of proteins.[40] The significantly darker and uniformly blue fibrous membranes from reaction with genipin at 65 °C for merely 1 h provided clear evidence of cross-linking and were further studied.

None of the bonds expected from genipin cross-linking reactions could be discerned on the Fourier transform infrared (FTIR)−attenuated total reflection (ATR) spectra (Figure S2) because of their overlapping with C−N and C−O stretch of SPs and PVA at 1090 cm^{-1} and genipin characteristic peaks at 1443 and 1080 cm^{-1} (Figure 2a). Whereas the heat-treated membrane exhibited a significantly reduced peak at 3362 cm^{-1} (N−H and O−H stretchings, Figure 2a), consistent with the

DOI: 10.1021/acsomega.9b03242
ACS Omega 2020, 5, 634−642

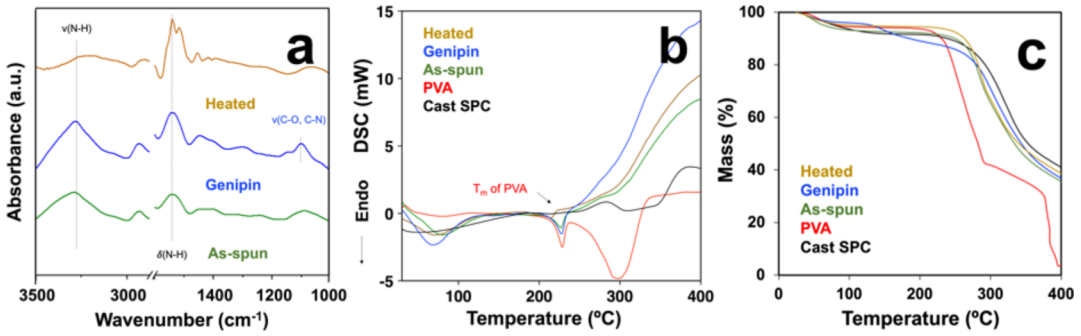

Figure 2. Characterization of SPC/PVA (7:3, 9%) as-spun, genipin-cross-linked (65 °C, 1 h), and heated (150 °C, 12 h) fibrous membranes: (a) FTIR−ATR spectra; (b) DSC; (c) TGA.

amidation and esterification of the $-NH_2$, −COOH, and −OH among SPs and possibly esterification between SPs and PVA. Analyses of FTIR amide I bonds in fibers electrospun from SPC as well as those reacted with genipin or heat-treated all showed very high extents (86−89%) of the ordered α-helix and β domains, 18−21% higher than those electrospun from pH adjusted then heated SP suspensions (not shown). X-ray diffraction diagrams also confirmed that all fibrous membranes were similarly semicrystalline with the crystalline index (CrI) of 60.8−66.8% (Figure S3, Table S2).

A similar PVA melting endotherm (ca. 227 °C, 30−45 J/g) was observed in as-spun and genipin-reacted fibrous membranes as in electrospun PVA (228 °C, 55 J/g), but with lowered endotherm and broad exotherms above 210 °C (Figure 2b,c, Table S3). The peak decomposition temperature in both genipin (298 °C)- and heat (287 and 313 °C)-treated samples was distinctively higher than that of as-spun membranes (284 °C), indicating the improved thermal stability, although their weight losses at 400 °C were similar (52−57%, Figures 2c and S3, Table S3). These data confirmed both genipin reaction (65 °C, 1 h) and heat treatments (150 °C, 12 h) improved thermal stability of the hybrid membranes.

Stability in Water. The stability of these fibrous membranes in water was observed by their mass and morphology (Figure 3). The as-spun fibrous membranes lost substantial mass (36.9%) after 1 d and only 1.4% more after prolonged 14 d exposure (Figure 3a, Table S4). The water-immersed membrane remained opaquely white after lyophilization, but fibers deformed and merged (Figure 3a, Table S4). The genipin-reacted membrane lost less mass (21.5% after 14 d) and more gradually, that is, 10.8% after 1 d and another 10.7% after 14 d (Table S4), and appeared pale blue with merged fibers upon lyophilization, evident of reactions between genipin and SP amines but some loss of genipin (Figure 3b, Table S4). In contrast, the heat-treated membrane only lost 5.4% weight after 14 d in water and retained the same fiber morphology except for ca. 20% wider fibers (277 ± 36 nm, N = 100) (Figure 3c). Most impressively, the heat-treated fibers remained essentially unchanged morphologically from extended 2 d immersions in strong acid (1 M HCl, pH 0) or base (0.0001 M NaOH, pH 10) and only slightly deformed from boiling for 2 h, all while losing 8.9−12.4% mass (Figure 3d−f). Such water resiliency was further examined by shearing the heat-treated membrane into single fibers by high-speed blending (30k rpm, 1 min) and then air-dried (AD) to be imaged by atomic force microscopy (AFM) to show excellent shape retention from shear force. The average root-mean-square roughness of 118 ± 24 nm (N = 5, Figure S4), corresponding to the aggregated SPs and the desirable higher specific surface for sorption applications. The excellent integrity of heated fibers following prolonged aq. immersions under extreme pH and at boil or strong shear force confirms the effectiveness of heat-induced condensation among SPs and between SPs and PVA. The 5.4−12.4% mass losses from the heat-treated were likely because of the unbonded PVA. Clearly, the impressive aqueous stability and resiliency of the heat-treated SP fibers are superior over all those reported by others.[26−32]

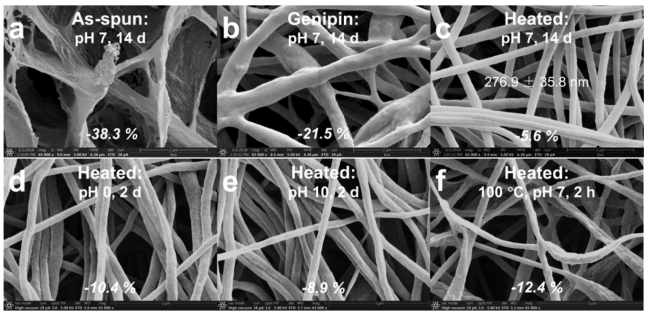

Figure 3. SEM images of electrospun SPC/PVA (7:3, 9%) fibrous membranes lyophilized after water immersion under different conditions and lengths of time: (a) as-spun; (b) genipin-crosslinked (65 °C, 1 h); (c−f) heated (150 °C, 12 h). Mass loss values in % (N = 3) are denoted.

Color Change in Wet and Dry States. The as-spun fibrous membranes appeared opaquely white, became translucent and gel-like when wet by water, and then translucent pale yellow and film-like when AD, losing most of fibrous features (Figure S5). Both genipin and heat-treated SPC/PVA fibrous membranes showed remarkable changes in colors and color strength (CS) when saturated with water (Figure 4a,b). The genipin-reacted membrane turned from pale blue (CS = 36) into dark blue (CS = 394) once wet by water and remained dark blue (CS = 330) when AD into a thin film (Figure 4a−c, Table S5). The heat-treated membranes were khaki (Ch = 9) in color and became orange (CS = 98) when wet and then reversed back to similarly khaki (CS = 15) when air dried (Figure 4a,b,d, Table S5). Therefore, the color changes to the respective orange and dark blue colors of both genipin and heat-treated membranes can signal the presence of water, but only the heated membrane remained fibrous and could return to the original color upon air-drying, reversible for a few times, giving another clear evidence of sufficient cross-

DOI: 10.1021/acsomega.9b03242
ACS Omega 2020, 5, 634−642

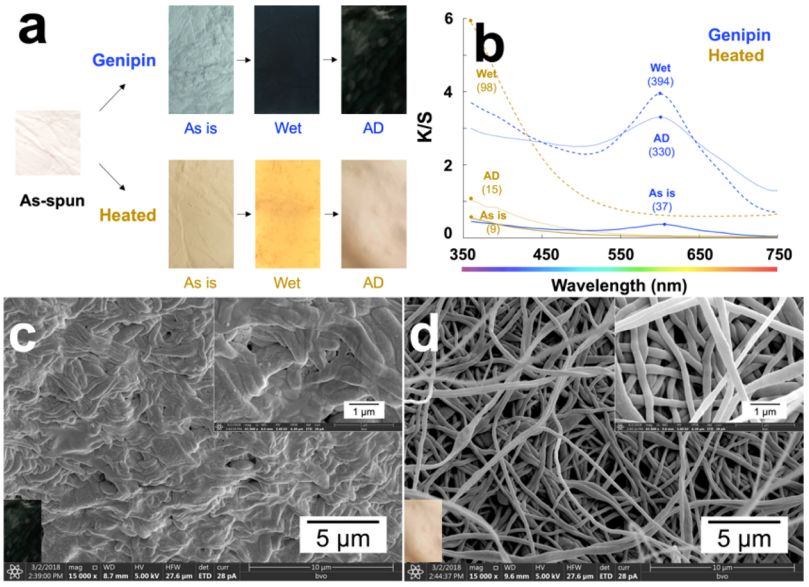

Figure 4. As-spun, genipin-crosslinked (65 °C, 1 h), and heated (150 °C, 12 h) SPC/PVA (7:3, 9%) fibrous membranes: (a) photographs of as is, wet, and AD; (b) *K*/*S* values with CS denoted in (); (c,d) SEM images of AD genipin-crosslinked and heated membranes.

Table 1. Liquid CA and Absorption of As-Spun and Heat-Treated Membranes (N = 5)

				as-spun			heated		
liquid	surface tension (mN/m)	dielectric constant	density (g/cm^3)	CA (deg)	mL/g	g/g	CA (deg)	mL/g	g/g
water	72.8	80.3	0.997	39.2 (±1.6)	21.2 (±0.7)	21.1 (±0.7)	110.5 (±6.4)	20.5 (±1.6)	20.4 (±1.6)
toluene	28.4	2.4	0.867	0	7.1 (±0.7)	6.2 (±0.6)	0	15.5 (±2.2)	13.4 (±1.9)
hexadecane	27.5	2.1	0.770	0	8.8 (±0.9)	6.8 (±0.7)	0	23.4 (±4.4)	18.0 (±3.4)
octane	21.6	2.0	0.703	0	9.4 (±1.1)	6.6 (±0.8)	0	16.2 (±2.4)	11.4 (±1.7)

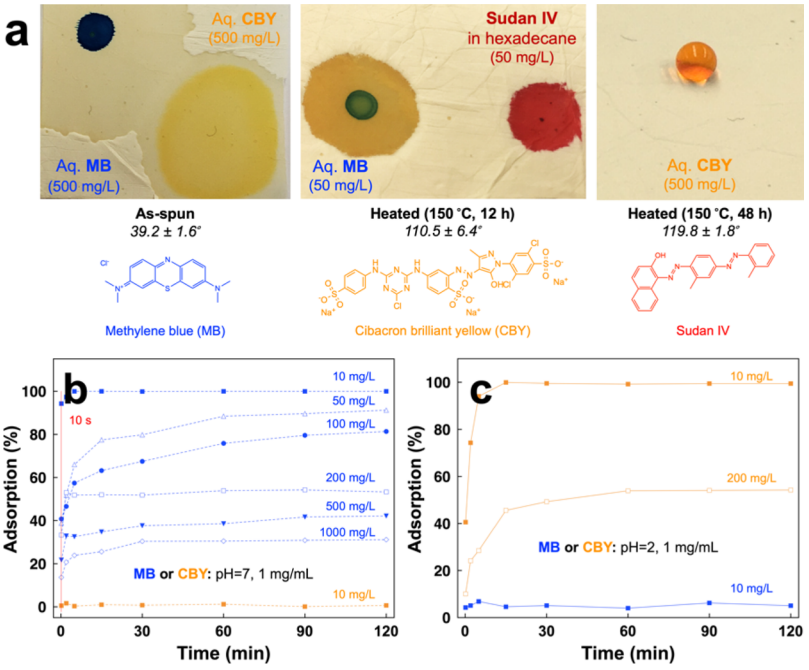

Figure 5. Dye wetting and absorption on heat-treated electrospun SPC/PVA (7:3, 9%) fibrous membranes: (a) aqueous MB and CBY (500 mg/L), and Sudan IV in hexadecane (50 mg/L) with the average water CA denoted (N = 5); adsorption of MB (blue) and CBY (orange) at the 1 mg/mL membrane to solution ratio over time: (b) at pH 7 and (c) at pH 2.

DOI: 10.1021/acsomega.9b03242
ACS Omega 2020, 5, 634−642

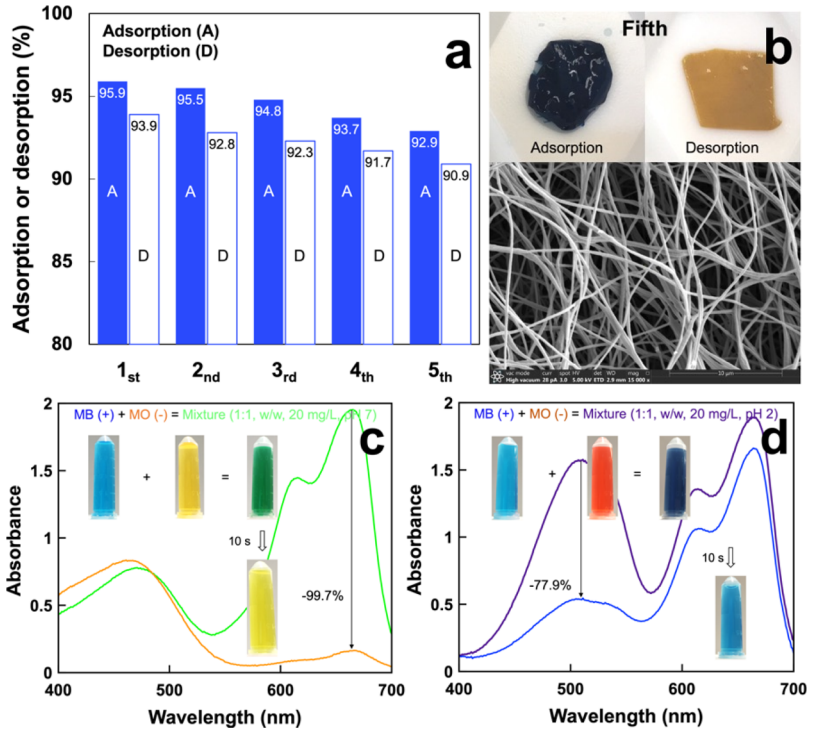

Figure 6. Repetitive and selection dye adsorption on electrospun SPC/PVA (7:3, 9%) heat-treated (150 °C, 12 h) fibrous membranes (100 mg) at fixed 1 mg/mL membrane/dye ratio: (a) five repetitive MB (20 mg/L) adsorption (pH 7) and desorption (pH 2) cycles; (b) photographs and scanning electron microscope (SEM) images of membranes after the fifth cycle; (c) images and UV−vis spectra of MB/MO mixture (1:1, 20 mg/L) before and after selective adsorption of MB at pH 7; (d) that of MO at pH 2.

linking and water stability of the heat-treated fibrous membranes.

Rapid and Selective Adsorption and Desorption of Ionic Dyes. The as-spun membranes were hydrophilic, having an average water contact angle (CA) of 39.2° and absorbing 21.2 ± 0.7 mL/g (N = 5) water, while even more readily wettable by nonpolar toluene, hexadecane, and octane but absorbing much less (7.1−9.4 mL/g) of these low-surface tension liquids and lost almost no mass (Table 1). The as-spun membranes were clearly amphiphilic on their surfaces but more hydrophilic in the bulk and in fact partially water soluble, losing over one-third of mass and fibrous structures as observed earlier. The 12 h heat-treated membrane surface became significantly hydrophobic with an average water CA of 110.5° (Table 1), while the bulk of the membrane remained amphiphilic, absorbing similar quantities of both water (20.5 mL/g) and nonpolar solvents (15.5−23.4 mL/g) (Table 1). The heat-induced hydrophobicity is consistent with dehydration reactions among polar −OH, −COOH, and $-NH_2$ groups into less polar amide and nonpolar esters. Lengthening the heat treatment to 48 h only slightly increased the water CA to 119.8 ± 1.8°, indicating slightly further condensations.

Wetting and adsorption of aq. cationic methylene blue (MB) and anionic CBY as well as lipophilic Sudan IV in hexadecane of the fibrous membranes behaved differently under the neutral condition. Aq. MB and CBY droplets (10 μL) wetted the as-spun membrane within 3−5 s and water in both dye solutions spread to wet larger areas than the initial droplets. However, cationic MB only colored the original footprint of the droplet whereas anionic CBY spreads nearly to the edge of the wetted area (Figure 5a). This swift affinity of cationic MB over the anionic CBY to the as-spun membrane indicates its more negatively charged nature. The heat-treated membrane also showed similarly higher affinity to cationic MB than anionic CBY (not shown) but took longer to wet, that is, 10 s or a few minutes for that heated for 12 or 48 h, respectively, indicative of the increased hydrophobicity while remaining more negatively charged. The one heated for 48 h even caused the aq. CBY to bead up (Figure 5a, right) but insufficiently hydrophobic to adsorb lipophilic Sudan IV in hexadecane.

The pH-dependent amphoteric characteristics of the heat-treated fibrous membranes were further demonstrated by respective adsorption of cationic MB and anionic CBY under neutral and acidic (pH 2) conditions. At pH 7, above the 4.5 PI of SPs, the fibrous membrane was negatively charged and adsorbed cationic MB rapidly to remove 94.3% from the 10 mg/L mixture in 10 s but adsorbed only 9.9% CBY (Figure 5b). At pH 2, 94.0% of anionic CBY in the 10 mg/L mixture was adsorbed in 5 min while only 6.2% MB was adsorbed (Figure 5c). The distinct pH-dependent and switchable electrostatic binding preference toward ionic species of the heated membrane is attributed to deprotonation of −COOH at neutral or protonation of $-NH_2$ groups at pH 2, that is, above and below the PI. With increasing initial MB concentrations of 50, 100, 200, and 1000 mg/L, the MB absorbed decreased, that is, 91.3, 81.4, 54.2, and 31.1%, respectively, and leveled off after 15 min at lower 10−200 mg/L and 30 min at higher 500−1000 mg/L concentrations (Figure 5b). Total MB adsorbed increased with initial 10−1000 mg/L concentrations, that is, from 10.5 to 311.3 mg per g of fibrous membrane (Figure S6). In the case of anionic CBY (200 mg/L), the total removal (54.0%) at pH 2 was similar to that of cationic MB (54.2%) at pH 7 but reaching equilibrium over much longer time of 60 min (Figure 5c). While the maximum adsorption capability (312.5 mg/g, pH 7) of heat-treated (12 h) fibrous membranes (Figure S6) is similar to

DOI: 10.1021/acsomega.9b03242
ACS Omega 2020, 5, 634−642

values reported on some activated carbons (9.8−980 mg/g, 0.1−1 h), the most significant distinction is in its short 0.5 h time to reach equilibrium, far shorter than fibers electrospun from other proteins and/or synthetic polymers,[11−13] that is, 6 h by keratin (170 mg/g, pH 6),[11] 2 h by sericin/β-cyclodextrin/PVA (2:1:7, 187 mg/g, pH 8),[12] and 6 h by β-cyclodextrin/poly(acrylic acid) (5:1, 826 mg/g, pH 9)[13] and most agricultural and industrial wastes (0.84−472.1 mg/g, ca. 0.5−24 h).[45]

The MB adsorption data on heat-treated membranes showed a significantly higher correlation coefficient R^2 values of >0.99 in Ho's pseudo-second-order model (Figure S7) than the merely 0.47−0.70 in Lagergren's pseudo-first-order model (not shown). Therefore, the overall MB adsorption is confirmed to be by chemisorption instead of physisorption. The adsorbed MB quantities also showed a better fit of Freundlich isotherm with the R^2 of 0.9879 (Figure S7) over the Langmuir isotherm (R^2 = 0.9269) to support more heterogeneous adsorption of MB onto the fiber surfaces where −COOH and $-NH_2$ groups are randomly distributed.

The five cyclic MB desorption−desorption of heat-treated membranes showed that 93−97% was adsorbed in 5 min and 91−94% of MB desorbed within 1 min, turning the dark blue membrane into the original dark yellow color (Figure 6a,b). MB adsorption and desorption were over 90% in all 5 cycles while the membranes retained their fibrous morphologies (Figure 6a,b), validating the feasibility of recovering MB and regenerating membranes for practical repetitive adsorption/desorption applications.

Under neutral condition, it took only 10 s for the anionically charged membrane to remove 99.7% of the cationic MB from the 1:1 MB/methyl orange (MO) mixtures, turning the clover green mixture into lemon yellow and leaving 89.9% anionic MO (Figure 6c). At pH 2, the positively charged fibrous membranes selectively adsorbed 77.9% anionic MO within 10 s, leaving a blue solution containing 79.7% MB (Figure 6d). While selective adsorption took only seconds in both cases, low extents of the oppositely charged dyes, that is, ca. 10% MO and 20% MB, were also adsorbed in the due process, indicating very high but not absolute selectivity. Nevertheless, the unique pH-dependent amphoteric characteristics as demonstrated by selective binding of cationic and anionic dyes demonstrate the potential of these SP fibrous membranes for applications in separation and recovery of oppositely charged ionic species.

CONCLUSIONS

Homogeneous and stable aq. SPCs have been facilely produced by high-speed blending (30k rpm, 15 min) and robustly electrospun into SP-rich fibrous membranes of uniform ultrafine fibers in 231 nm average. These SP-rich fibrous membranes can be rendered water-insoluble with either genipin reaction or heat treatment. The heat-treated membranes, in particular, exhibit excellent wet resiliency under prolonged exposure (pH 7, 14 d), extremely acidic (pH 0, 2 d) and basic (pH 10, 2 d) conditions, and at boil (2 h) and from high shear force (30k rpm, 1 min). This successful shear force process to generate aq. SPCs for electrospinning and heat condensation to fabricate wet-resilient fibrous membranes represents the first green approach for globular proteins without chemicals such as alkali, urea, or surfactants as reported by others. Furthermore, these amphoteric SP-rich fibrous membranes can be simply deprotonated to carry negative charges under neutral or protonated to be positively charged under acidic (pH 2) conditions to selectively adsorb respective cationic MB or anionic CBY and MO dyes via electrostatic interactions. The rapid MB adsorption fits the pseudo-second-order kinetics model and Freundlich adsorption isotherm to affirm chemisorption mechanism and the chemically heterogeneous nature of the fiber surfaces. The absorbed dyes can be effectively desorbed to regenerate the wet-resilient fibrous membranes in five adsorption/desorption cycles. This demonstrated ability to selectively separate and recover cationic and anionic dyes that can be expanded in the separation and recovery of other cationic and/or anionic compounds relevant to many potential environmental, biological, and industrial applications.

EXPERIMENTAL SECTION

Materials. SPI (92% protein) was from MP Biomedicals, LLC. Urea (98.0%, ACS reagent grade), PVA (146−186 kDa, 87−89% hydrolyzed), cibacron brilliant yellow 3G-P (CBY), and Sudan IV red were purchased from Aldrich Chemical Company. Hydrochloric acid (HCl, 1 N, certified), sodium hydroxide (NaOH, 1 N, certified), ethanol (EtOH, histological grade), hexadecane (certified), toluene (certified), chloroform (certified), and MB were obtained from Fisher Scientific. Genipin (98%, HPLC grade) was purchased from Wako Pure Chemical Industries, Ltd., and MO was purchased from EMD Chemicals. All chemicals were used as received. All aq. solutions and suspensions were prepared with water purified by the Millipore Milli-Q plus water purification system.

Electrospinning. Aq. SP suspensions were prepared by adding 9% crude SPI in water under constant magnetically stirring for 1 h at ambient temperature, followed by either adjusting the pH to 12 using 1 M NaOH and then heated at 90 °C for 45 min or treating in the opposite order. Aq. SPC was the supernatant from blending 9% SP suspensions at 30k rpm for 15 min using a high-speed blender (Vitamix 5200), cooled to ambient temperature, and then centrifuged at 5k rpm for 15 min. Aq. PVA solutions were prepared at 9 or 12% by heating at 95 °C for 6 h under constant stirring and then cooled to ambient temperature. All concentrations were in wt % and expressed as % throughout.

Electrospinning was performed using mixtures of either magnetically stirred (ca. 2k rpm, 1 h) 9% SP suspension or SPC with 9% PVA at 1:1, 7:3, and 9:1 w/w ratios. Each mixture was loaded into a 30 mL horizontally placed syringe (Popper & Sons, Inc.), fed at 0.01−2 mL/h using a syringe pump (KDS 200, KD Scientific, USA) through a flat-end metal needle (21 gauge), and electrospun at 15 kV operated with a dc power supply (ES 30-0.1 P, Gamma High Supply, USA). The fine fibrous membranes were collected on a vertically placed aluminium foil (30 cm × 30 cm) at 25 cm from the needle tip to reach a typical thickness of 150−200 μm.

Genipin Cross-linking and Heat Treatment. Electrospun SPC/PVA (7:3, 9%) fibrous membranes (ca. 100 mg) were chemically reacted with genipin or heat-treated to improve aq. stability. Chemical cross-linking with 11 mM genipin in 1:1 v/v EtOH/water was performed by either complete submersion in genipin in an open Petri dish to expose to ambient oxygen for 24 h or saturation with ca. 600 mg genipin solutions in a sealed centrifuge tube at 65 °C for 1 h. Following each process, the membrane was thoroughly washed with EtOH and water in sequence, frozen at −20 °C for 1 h, and then lyophilized at −50 °C for 24 h in a freeze-drier (free zone 1.0 L Benchtop Freeze Dry System, Labconco,

DOI: 10.1021/acsomega.9b03242
ACS Omega 2020, 5, 634−642

Kansas City, MO). Electrospun SPC/PVA (7:3, 9%) fibrous membranes were heated at 150 °C under vacuum (ca. 20 Hg) for 12 or 48 h and cooled to ambient temperature.

Characterizations. The morphologies of as-spun and cross-linked electrospun SPC/PVA (7:3, 9%) fibrous membranes were observed using a field-emission SEM (XL 30-SFEG, FEI/Philips, USA; Quattro, Thermo Scientific, USA) at a working distance of ca. 5 mm and an accelerating voltage of 5 kV. Each sample was mounted with conductive carbon tapes and sputter-coated with gold/palladium before imaging. Widths of fibers were measured from 100 individual fibers, and the mean and standard deviation were reported. Heated (12 h) membranes were blended (30k rpm, 1 min) in water at 0.1% and AD on the freshly peeled mica (highest grade V1 mica discs, 15 mm, Ted Pella, Inc.). Then, both Leica DM2500 optical microscope equipped with the cross-polarizing filter and AFM (MFP-3D, Oxford Instruments Asylum Research, Inc., Santa Barbara, CA) were applied for the imaging. AFM scanned in the tapping mode with OMCL-AC160TS standard silicon probes (tip radius < 10 nm, spring constant = 28.98 N/m, resonant frequency of ca. 310 kHz, Olympus Corp.) at 1 Hz scan rate under the ambient condition.

The chemical composition and secondary structures of SPs in fibrous membranes were studied by FTIR−ATR spectra collected from 3500 to 1000 cm^{-1} at a resolution of 2 cm^{-1} using a Nicolet iN10 microscope spectrometer (Thermo Fisher Scientific, USA) equipped with a liquid nitrogen-cooled detector. The secondary structure composition, including α-helix (1645−1662 cm^{-1}), β-sheet (1613−1637, 1682−1689 cm^{-1}), β-turn (1662−1682 cm^{-1}), and random coil (1637−1645 cm^{-1}),[39] was analyzed in the range of 1600−1700 cm^{-1} as reported in our prior work.[32] X-ray diffraction (XRD) patterns were collected to study the crystalline structures of SPC cast film and electrospun PVA and hybrid fibers on a Scintag XDS 2000 powder diffractometer using a Ni-filtered Cu Kα radiation (=1.5406 Å) at an anode voltage of 45 kV and a current of 40 mA. Samples were compressed into 1 mm thick flat sheets between two glass slides, and diffractograms were recorded from 5 to 40° at a scan rate of 2°/min. Peak deconvolution analysis was conducted using Peak Fit (Systat Software), and individual peaks were fitted by Gaussian functions with $R^2 > 0.99$ for all deconvolutions. The ratio of the total crystalline peak area and the sum of both crystalline and amorphous area was taken as the crystallinity index (CrI).

Thermal behavior of SPC cast film and electrospun membranes was measured using a Shimadzu thermal analysis system (TA-SOWSI), including a differential scanning calorimeter (DSC-60) and a thermogravimetric analyzer (TGA-50). Both DSC and TGA were performed by heating at 10 °C/min under flowing N_2 at a 50 mL/min rate to 400 °C. The first derivative was derived from the TGA data and plotted as the derivative thermogravimetric (DTG) curve. The L* (lightness), a* (red to green) and b* (yellow to blue) color coordinates and K/S (absorption/scattering) values of as-spun and crosslinked hybrid fibrous membranes were measured using a Gretag Macbeth Color-Eye 7000A tester (Akron, Ohio, United States). All samples were sandwiched between two glass slides, measured at four different locations, and the average is reported. K/S values were calculated by the Kubelka−Munk equation based on the spectral reflectance (R in %) of the samples as

$$\frac{K}{S} = \frac{(1-R)^2}{2R}$$

The CS was calculated by using the as-spun hybrid membrane as the standard

$$\text{Color strength (CS)} = [(K/S)_{\text{sample}}/(K/S)_{\text{standard}}] \times 100\ \%$$

The dry mass of each membrane before and after immersion in aq. media with pH of 0−10 for 1−14 d and air-drying at 65 °C was measured to 0.01 mg using an analytical balance (Shimadzu, AUW220D). Water CA (10 μL) on the surface of fibrous membranes was measured by the drop shape analysis method before the spreading of water droplets. Each membrane was measured five times in different locations to derive the average and standard deviation. The liquid (water, toluene, hexadecane, and octane, $N = 5$) uptake of the as-spun and heat-treated (12 h) membrane was also weighed to report the average and standard deviation. The length, width, and thickness swelling of the heat-treated membrane immersed in water for up to 2 h were determined by measuring with a vernier scale to the nearest 0.01 mm.

Adsorption and Desorption. The adsorption of cationic MB or anionic CBY on heat-treated (12 h) 7:3 SPC/PVA fibrous membrane was carried out by immersing ca. 100 mg adsorbent in 100 mL aq. MB (10−1000 mg/L) at pH 7 or CBY (10−200 mg/L) at pH 2 at ambient temperature, handshaking for 10 s then in a shaker (100−150 rpm) for up to 2 h. At predetermined time intervals, 0.5 mL solution was taken to quantify the amount of MB or CBY using an Evolution 600 UV−vis spectrophotometer (Thermo Scientific) based on the calibration curve determined in the same aq. media. The percentage of MB or CBY removal was calculated as

$$\text{Percentage of removal} = \frac{C_0 - C}{C_0} \times 100\%$$

where C_0 and C is the initial and current dye concentration, respectively. The amount of MB or CBY adsorbed at each time interval on the membrane, q (in mg/g), was calculated as

$$q = \frac{(C_0 - C) \times V}{m}$$

where V is the solution volume, and m is the mass of the membranes. The adsorption kinetics of MB on heat-treated membranes, that is, t/q_t (q_t, quantity adsorbed at time t) versus t plot, was fitted with both Lagergren's pseudo-first-order[41] and Ho's pseudo-second-order[42] models for physisorption and chemisorption, respectively, as well as Freundlich[43] and Langmuir[44] isotherms, typical of adsorption to heterogeneous and homogeneous surfaces, respectively. The recovery of MB and regeneration of the fibrous membrane (ca. 100 mg) was conducted in five repetitive adsorption/desorption cycles of 5 min adsorption of MB (20 mg/L, 100 mL) at pH 7 and 1 min desorption of MB at pH 2. Following each adsorption/desorption cycle, the membrane was thoroughly washed by acid (pH 2) and then neutralized for the next cycle. The adsorption efficiency was evaluated based on dyes left in the solution, and the desorption efficiency was derived from the dyes recovered. Selective absorption of either cationic MB or anionic MO dye from 100 mL 1:1 w/w MB/MO mixture (20

DOI: 10.1021/acsomega.9b03242
ACS Omega 2020, 5, 634−642

mg/L) was studied at pH 7 and 2. Anionic MO was used in place of anionic CBY as CBY precipitated when mixed with MB.

■ ASSOCIATED CONTENT

Supporting Information

The Supporting Information is available free of charge at https://pubs.acs.org/doi/10.1021/acsomega.9b03242.

SEM images of electrospun SP/PVA fibrous membranes, genipin cross-linking and mechanism, FTIR−ATR, XRD, and DTG of as-spun and heated electrospun SPC/PVA fibrous membranes, AFM images of single fibers in heated membrane, dye adsorption capability, and model fittings (PDF)

■ AUTHOR INFORMATION

Corresponding Author

*E-mail: ylhsieh@ucdavis.edu.

ORCID

Xingchen Liu: 0000-0002-1011-5771

You-Lo Hsieh: 0000-0003-4795-260X

Notes

The authors declare no competing financial interest.

■ ACKNOWLEDGMENTS

The authors appreciate funding support from Henry A. Jastro Research Award, University of California, Davis and USDA National Institute of Food and Agriculture, Hatch project CA-D-6706H.

■ REFERENCES

(1) Robinson, T.; McMullan, G.; Marchant, R.; Nigam, P. Remediation of dyes in textile effluent: a critical review on current treatment technologies with a proposed alternative. *Bioresour. Technol.* **2001**, *77*, 247−255.

(2) Robinson, T.; Chandran, B.; Nigam, P. Removal of dyes from a synthetic textile dye effluent by biosorption on apple pomace and wheat straw. *Water Res.* **2002**, *36*, 2824−2830.

(3) Panic, V.; Seslija, S.; Nesic, A.; Velickovic, S. Adsorption of azo dyes on polymer materials. *Chem. Ind.* **2013**, *67*, 881−900.

(4) Shannon, M. A.; Bohn, P. W.; Elimelech, M.; Georgiadis, J. G.; Marinas, B. J.; Mayes, A. M. Science and technology for water purification in the coming decades. *Nanoscience and Technology: A Collection of Reviews from Nature Journals*; World Scientific, 2010; pp 337−346.

(5) Zhang, R.; Peng, H.; Zhou, T.; Li, M.; Guo, X.; Yao, Y. Selective Adsorption and Separation of Organic Dyes by Poly (acrylic acid) Hydrogels Formed with Spherical Polymer Brushes and Chitosan. *Aust. J. Chem.* **2018**, *71*, 846.

(6) Deng, S.; Xu, H.; Jiang, X.; Yin, J. Poly(vinyl alcohol) (PVA)-Enhanced Hybrid Hydrogels of Hyperbranched Poly(ether amine) (hPEA) for Selective Adsorption and Separation of Dyes. *Macromolecules* **2013**, *46*, 2399−2406.

(7) Molina, E. F.; Parreira, R. L. T.; De Faria, E. H.; de Carvalho, H. W. P.; Coimbra, G. F.; Nassar, E. J.; Ciuffi, K. J.; Ciuffi, K. J. Ureasil-Poly(ethylene oxide) Hybrid Matrix for Selective Adsorption and Separation of Dyes from Water. *Langmuir* **2014**, *30*, 3857−3868.

(8) Zhang, Y.; Ma, X.; Xu, H.; Shi, Z.; Yin, J.; Jiang, X. Selective Adsorption and Separation through Molecular Filtration by Hyperbranched Poly(ether amine)/Carbon Nanotube Ultrathin Membranes. *Langmuir* **2016**, *32*, 13073−13083.

(9) Zhang, C.; Li, P.; Huang, W.; Cao, B. Selective adsorption and separation of organic dyes in aqueous solutions by hydrolyzed PIM-1 microfibers. *Chem. Eng. Res. Des.* **2016**, *109*, 76−85.

(10) Zhu, Z.; Wu, P.; Liu, G.; He, X.; Qi, B.; Zeng, G.; Wang, W.; Sun, Y.; Cui, F. Ultrahigh adsorption capacity of anionic dyes with sharp selectivity through the cationic charged hybrid nanofibrous membranes. *Chem. Eng. J.* **2017**, *313*, 957−966.

(11) Aluigi, A.; Rombaldoni, F.; Tonetti, C.; Jannoke, L. Study of Methylene Blue adsorption on keratin nanofibrous membranes. *J. Hazard. Mater.* **2014**, *268*, 156−165.

(12) Zhao, R.; Wang, Y.; Li, X.; Sun, B.; Jiang, Z.; Wang, C. Water-insoluble sericin/β-cyclodextrin/PVA composite electrospun nanofibers as effective adsorbents towards methylene blue. *Colloids Surf., B* **2015**, *136*, 375−382.

(13) Zhao, R.; Wang, Y.; Li, X.; Sun, B.; Wang, C. Synthesis of β-Cyclodextrin-Based Electrospun Nanofiber Membranes for Highly Efficient Adsorption and Separation of Methylene Blue. *ACS Appl. Mater. Interfaces* **2015**, *7*, 26649−26657.

(14) Zohuriaan-Mehr, M. J.; Kabiri, K. Superabsorbent polymer materials: a review. *Iran. Polym. J.* **2008**, *17* (6), 451−477.

(15) Kim, H.-R.; Jang, J.-W.; Park, J.-W. Carboxymethyl chitosan-modified magnetic-cored dendrimer as an amphoteric adsorbent. *J. Hazard. Mater.* **2016**, *317*, 608−616.

(16) Xu, S.; Wang, J.; Wu, R.; Wang, J.; Li, H. Adsorption behaviors of acid and basic dyes on crosslinked amphoteric starch. *Chem. Eng. J.* **2006**, *117*, 161−167.

(17) Zhang, W.; Yang, H.; Dong, L.; Yan, H.; Li, H.; Jiang, Z.; Kan, X.; Li, A.; Cheng, R. Efficient removal of both cationic and anionic dyes from aqueous solutions using a novel amphoteric straw-based adsorbent. *Carbohydr. Polym.* **2012**, *90*, 887−893.

(18) Zhou, Y.; Hu, Y.; Huang, W.; Cheng, G.; Cui, C.; Lu, J. A novel amphoteric β-cyclodextrin-based adsorbent for simultaneous removal of cationic/anionic dyes and bisphenol A. *Chem. Eng. J.* **2018**, *341*, 47−57.

(19) Fan, Y.; Liu, H.-J.; Zhang, Y.; Chen, Y. Adsorption of anionic MO or cationic MB from MO/MB mixture using polyacrylonitrile fiber hydrothermally treated with hyperbranched polyethylenimine. *J. Hazard. Mater.* **2015**, *283*, 321−328.

(20) Riblett, A. L.; Herald, T. J.; Schmidt, K. A.; Tilley, K. A. Characterization of β-Conglycinin and Glycinin Soy Protein Fractions from Four Selected Soybean Genotypes. *J. Agric. Food Chem.* **2001**, *49*, 4983−4989.

(21) Tian, K.; Shao, Z.; Chen, X. Natural electroactive hydrogel from soy protein isolation. *Biomacromolecules* **2010**, *11*, 3638−3643.

(22) *Foreign Agricultural Service Report, Oil seeds: World Market and Trade*; U.S. Department of Agriculture, 2018.

(23) Li, M.; Mondrinos, M. J.; Gandhi, M. R.; Ko, F. K.; Weiss, A. S.; Lelkes, P. I. Electrospun protein fibers as matrices for tissue engineering. *Biomaterials* **2005**, *26*, 5999−6008.

(24) Jin, H.-J.; Fridrikh, S. V.; Rutledge, G. C.; Kaplan, D. L. ElectrospinningBombyx moriSilk with Poly(ethylene oxide). *Biomacromolecules* **2002**, *3*, 1233−1239.

(25) Xu, X.; Jiang, L.; Zhou, Z.; Wu, X.; Wang, Y. Preparation and properties of electrospun soy protein isolate/polyethylene oxide nanofiber membranes. *ACS Appl. Mater. Interfaces* **2012**, *4*, 4331−4337.

(26) Har-el, Y.-e.; Gerstenhaber, J. A.; Brodsky, R.; Huneke, R. B.; Lelkes, P. I. Electrospun soy protein scaffolds as wound dressings: Enhanced reepithelialization in a porcine model of wound healing. *Wound Med.* **2014**, *5*, 9−15.

(27) Vega-Lugo, A.-C.; Lim, L.-T. Electrospinning of soy protein isolate nanofibers. *J. Biobased Mater. Bioenergy* **2008**, *2*, 223−230.

(28) Fang, Q.; Zhu, M.; Yu, S.; Sui, G.; Yang, X. Studies on soy protein isolate/polyvinyl alcohol hybrid nanofiber membranes as multi-functional eco-friendly filtration materials. *Mater. Sci. Eng., B* **2016**, *214*, 1−10.

(29) Cho, D.; Nnadi, O.; Netravali, A.; Joo, Y. L. Electrospun Hybrid Soy Protein/PVA Fibers. *Macromol. Mater. Eng.* **2010**, *295*, 763−773.

(30) Xu, H.; Cai, S.; Sellers, A.; Yang, Y. Intrinsically water-stable electrospun three-dimensional ultrafine fibrous soy protein scaffolds

DOI: 10.1021/acsomega.9b03242
ACS Omega 2020, 5, 634−642

for soft tissue engineering using adipose derived mesenchymal stem cells. *RSC Adv.* **2014**, *4*, 15451−15457.
(31) Salas, C.; Ago, M.; Lucia, L. A.; Rojas, O. J. Synthesis of soy protein-lignin nanofibers by solution electrospinning. *React. Funct. Polym.* **2014**, *85*, 221−227.
(32) Liu, X.; Hsieh, Y.-L. Amphiphilic and amphoteric aqueous soy protein colloids and their cohesion and adhesion to cellulose. *Ind. Crops Prod.* **2020**, *144C*, 112041−112049.
(33) Chang, W.-H.; Chang, Y.; Lai, P.-H.; Sung, H.-W. A genipin-crosslinked gelatin membrane as wound-dressing material: in vitro and in vivo studies. *J. Biomater. Sci., Polym. Ed.* **2003**, *14*, 481−495.
(34) Frohbergh, M. E.; Katsman, A.; Botta, G. P.; Lazarovici, P.; Schauer, C. L.; Wegst, U. G. K.; Lelkes, P. I. Electrospun hydroxyapatite-containing chitosan nanofibers crosslinked with genipin for bone tissue engineering. *Biomaterials* **2012**, *33*, 9167−9178.
(35) Panzavolta, S.; Gioffrè, M.; Focarete, M. L.; Gualandi, C.; Foroni, L.; Bigi, A. Electrospun gelatin nanofibers: Optimization of genipin cross-linking to preserve fiber morphology after exposure to water. *Acta Biomater.* **2011**, *7*, 1702−1709.
(36) Lie; Gao, C.; Mao, Z.; Shen, J.; Hu, X.; Han, C. Thermal dehydration treatment and glutaraldehyde cross-linking to increase the biostability of collagen-chitosan porous scaffolds used as dermal equivalent. *J. Biomater. Sci., Polym. Ed.* **2003**, *14*, 861−874.
(37) Bellincampi, L. D.; Dunn, M. G. Effect of crosslinking method on collagen fiber-fibroblast interactions. *J. Appl. Polym. Sci.* **1997**, *63*, 1493−1498.
(38) Yannas, I. V.; Tobolsky, A. V. Cross-linking of gelatine by dehydration. *Nature* **1967**, *215*, 509−510.
(39) Touyama, R.; Inoue, K.; Takeda, Y.; Yatsuzuka, M.; Ikumoto, T.; Moritome, N.; Shingu, T.; Yokoi, T.; Inouye, H. Studies on the blue pigments produced from genipin and methylamine 0.2. On the formation mechanisms of brownish-red intermediates leading to the blue pigment formation. *Chem. Pharm. Bull.* **1994**, *42*, 1571.
(40) Rafatullah, M.; Sulaiman, O.; Hashim, R.; Ahmad, A. Adsorption of methylene blue on low-cost adsorbents: A review. *J. Hazard. Mater.* **2010**, *177*, 70−80.
(41) Goormaghtigh, E.; Cabiaux, V.; Ruysschaert, J.-M. Secondary structure and dosage of soluble and membrane proteins by attenuated total reflection Fourier-transform infrared spectroscopy on hydrated films. *Eur. J. Biochem.* **1990**, *193*, 409−420.
(42) Lagrergen, S. Zur Theorie Der Sogenannten Adsorption Gelöster Stoffe Kungliga Svenska Vetenskapsakademiens. *Handlingar* **1898**, *24* (4), 1−39.
(43) Ho, Y. S.; McKay, G. Pseudo-second order model for sorption processes. *Process Biochem.* **1999**, *34*, 451−465.
(44) Freundlich, H. Über die adsorption in lösungen. *Z. Phys. Chem.* **1907**, *57*, 385−470.
(45) Langmuir, I. The adsorption of gases on plane surfaces of glass, mica and platinum. *J. Am. Chem. Soc.* **1918**, *40*, 1361−1403.

DOI: 10.1021/acsomega.9b03242
ACS Omega 2020, 5, 634−642